

## Proceedings of the First International Conference on Medical Imaging and Case Reports (MICR-2018)

### Keynote Session

#### Expanding Frontiers of Neuroimaging: Dynamic Molecular Imaging

Rajendra D. Badgaiyan

*Department of Psychiatry, Icahn School of Medicine at Mount Sinai, New York, NY, USA*

#### Abstract

Lack of a sensitive method for detection of acute changes in neurotransmission has limited the scope of Neuroimaging research because neurotransmitters play an important role in regulation of cognitive and behavioral functions. We recently developed a technique to detect, map and measure dopamine released acutely during cognitive or behavioral processing. The technique is called Neurotransmitter imaging or Single scan dynamic molecular imaging technique (SDMIT). It exploits the competition between a neurotransmitter and its receptor ligand for occupancy of the same receptor site. In this technique after patients are positioned in the positron emission tomography (PET) camera, a radio-labeled neurotransmitter ligand is injected intravenously, and the PET data acquisition started. These data are used by a receptor kinetic model to detect, map and measure neurotransmitter released dynamically in different brain areas. Patients are asked to perform a cognitive task while in the scanner and the amount of neurotransmitter released in different brain areas measured. By comparing it with the data acquired in healthy volunteers during performance of a similar task, it is possible to determine whether a neurotransmitter release is dysregulated in the patients and whether the dysregulation is responsible for clinical symptoms. Since this technique measures neurotransmitter released under conditions of cognitive stress, it can detect changes at a very early stage, when dysregulation of is not expressed at rest but manifests under conditions of cognitive overload.

#### Neuroimaging Advances and Their Application to Schizophrenia and Mild Traumatic Brain Injury

Martha E. Shenton<sup>1-3\*</sup>, Marek Kubicki<sup>1,2</sup>, Sylvain Bouix<sup>1</sup>, Ofer Pasternak<sup>1,2</sup>, Yogesh Rathi<sup>1,2</sup>, Inga Koerte<sup>1,4</sup>, Michael Coleman<sup>1</sup>, Robert Stern<sup>5-7</sup> and Ross Zafonte<sup>8</sup>

<sup>1</sup>Psychiatry Neuroimaging Laboratory, Brigham and Women's Hospital, Harvard Medical School, Boston, MA, USA

<sup>2</sup>Department of Psychiatry and Radiology, Harvard Medical School, Boston, MA, USA

<sup>3</sup>VA Boston Healthcare System, Brockton, MA, USA

<sup>4</sup>Department of Child and Adolescent Psychiatry, Psychosomatics, and Psychotherapy, University Hospital, LMU Munich, Germany

<sup>5</sup>CTE Center, Boston University School of Medicine, Boston, MA, USA

<sup>6</sup>Alzheimer's Disease Center, Boston University School of Medicine, Boston, MA, USA

<sup>7</sup>Department of Anatomy, Neurology, and Neurosurgery, Boston University School of Medicine, Boston, MA, USA

<sup>8</sup>Department of Physical Medicine, Spaulding Rehabilitation Hospital, and Harvard Medical School, Boston, MA, USA

#### Abstract

Important advances in neuroimaging have revolutionized our understanding of the human brain. With these advances our ability to go beyond what was gleaned earlier only from post-mortem studies, has now elevated neuroimaging to a central role in neuroscience research and in clinical practice, where researchers are beginning to understand associations between brain and behavior in both healthy and impaired brains, and where clinicians routinely use such tools to assist in the diagnosis, staging, and follow up of disorders that affect the brain - all in a manner that was heretofore not possible. These advances became possible

only in the last three decades, beginning with structural imaging tools, and extending now to other imaging techniques that provide important new information about the brain. The focus of this presentation is to highlight advances in neuroimaging tools, most particularly diffusion imaging, and their application to quantifying brain abnormalities in schizophrenia and in mild traumatic brain injury. What these two disorders share in common is that the brain abnormalities are subtle and difficult to detect, and their quantification had to await the development of more advanced neuroimaging techniques. These advanced techniques, which continue to evolve, are important, and examples are provided of findings in schizophrenia and mild traumatic brain injury. We end with a discussion about the importance of method over theory at those times when speculations and theories can neither be tested nor confirmed without the advent of improved methods and tools, which make it possible to quantify important new information about the brain.

## AI, Machine Learning and Brain Clouds for Medical Imaging at 1mm Scales

**Michael I. Miller**

*Director of the Department of Biomedical Engineering, Johns Hopkins University, Baltimore, MD, USA*

### Abstract

I will review progress over the past two decades in Computational Anatomy and BrainGPS systems for coordinating Medical Imagery relative to emergent neurological atlases and the 1-millimeter scales. BrainGPS provides the opportunity for the next wave of high-throughput neuroinformatics in which Clouds of MR and functional imagery can be registered to anatomical standards for both precision medicine as well as cross-sectional, epidemiological studies. We will review the progress at Johns Hopkins University associated to MRI-Cloud for understanding neurodegenerative and neurodevelopmental diseases. Applications of machine learning and AI will be shown, including image retrieval, translation of MR pictures to diagnosis, risk prediction for conversion to disease, and generation of imaging and genomic phenotypes.

## Strategies for Decreasing Screening Mammography Recall Rates While Maintaining Performance Metrics

**Susan C. Harvey**

*Director of Breast Imaging, The Russell H. Morgan Department of Radiology and Radiological Science, JHM, Baltimore, MD, USA*

### Abstract

**Rationale and Objective:** This study aimed to determine the impact of interventions designed to reduce screening mammography recall rates on screening performance metrics.

**Materials and Methods:** We assessed baseline performance for full-field digital mammography (FFDM) and digital breast tomosynthesis mammography (DBT) for a 3-year period before intervention. The first intervention sought to increase awareness of recalls from screening mammography. Breast imagers discussed their perceptions regarding screening recalls and were required to review their own recalled cases, including outcomes of diagnostic evaluation and biopsy. The second intervention implemented consensus double reading of all recalls, requiring two radiologists to agree if recall was necessary. Recall rates, cancer detection rates, and positive predictive value 1 (PPV1) were compared before and after each intervention.

**Results:** The baseline recall rate, cancer detection rate, and PPV1 were 11.1%, 3.8/1000, and 3.4%, respectively, for FFDM, and 7.6%, 4.8/1000, and 6.0%, respectively, for DBT. Recall rates decreased significantly to 9.2% for FFDM and to 6.6% for DBT after the first intervention promoting awareness, as well as to 9.9% for FFDM after the second intervention implementing group consensus. PPV1 increased significantly to 5.7% for FFDM and to 9.0% for DBT after the second intervention. Cancer detection rate did not significantly change with the implementation of these interventions. An average of 2.3 minutes was spent consulting for each recall.

**Conclusion:** Reduction in recall rates is desirable, provided performance metrics remain favorable. Our interventions improved performance and could be implemented in other breast imaging settings.

## Machine Learning for Biomedical Data Analysis

**René Vidal**

*Department of Biomedical Engineering, Johns Hopkins University, Baltimore, MD, USA*

### Abstract

In this talk, I will overview our recent work on the development of automatic methods for the interpretation of biomedical data from multiple modalities and scales. At the cellular scale, I will present a structured matrix factorization method for segmenting neurons and finding their spiking patterns in calcium imaging videos, and a shape analysis method for classifying embryonic cardiomyocytes in optical imaging videos. At the organ scale, I will present a Riemannian framework for processing diffusion magnetic resonance images of the brain, and a stochastic tracking method for detecting Purkinje fibers in cardiac MRI. At the patient scale, I will present dynamical system and machine learning methods for recognizing surgical gestures and assessing surgeon skill in medical robotic motion and video data.

## Hippocampal Morphology Study based on Progressive Template Deformable Model

**Jinah Park<sup>1</sup>** and **Jaecil Kim<sup>2</sup>**

*<sup>1</sup>School of Computing, Korea Advanced Institute of Science and Technology, Republic of Korea*

*<sup>2</sup>Kyungpook National University, Republic of Korea*

### Abstract

Shape of an object can be represented by mesh structure consisting of nodes and their connections. We refer to such representation as a model incorporating its geometric degree of freedom to cover a family of the object. In this approach, we bring the morphometry study by representing the anatomical shape characteristics of human organs in a computational shape model. This talk presents the deformable modeling research work applied for various organ structures especially the hippocampus and ventricles of brain. For such application, it is important to robustly restore the individual shape details of the target structure as well as to build the anatomical point correspondences for shape comparisons. And it is also critical to decide what we want to measure from the model deformation intuitively. For shape analysis, we developed the template model of a target structure and a progressive template-to-image deformable registration in the shape modeling process. We share the results of our modeling applied to aging brain studies of collaborative work with a team at University of Edinburgh.

## Medical Image Imputation

**Polina Golland**

*Computer Science and Artificial Intelligence Laboratory, Massachusetts Institute of Technology, Cambridge, MA, USA*

### Abstract

We present an algorithm for creating high resolution anatomically plausible images that are consistent with acquired clinical brain MRI scans with large inter-slice spacing. Although large databases of clinical images contain a wealth of information, medical acquisition constraints result in sparse scans that miss much of the anatomy. These characteristics often render computational analysis impractical as standard processing algorithms tend to fail when applied to such images. Our goal is to enable application of existing algorithms that were originally developed for high resolution research scans to severely under sampled images. We illustrate the applications of the method in the context of neurodegeneration and white matter disease studies in stroke patients.

## Medical Imaging for Cell Therapy: Clinical Case Studies

**Jeff W. M. Bulte**

*Director of Cellular Imaging, The Johns Hopkins Institute for Cell Engineering, Baltimore, MD, USA*

### Abstract

Magnetic resonance (MR) imaging is expected to play a key role in evaluating the outcome of clinical trials based on

stem cell therapy. In order to facilitate and implement the translation of these therapies into the clinic, it will be necessary to monitor the immediate cellular engraftment, subsequent biodistribution and migration, and cell survival and differentiation non-invasively over time. This information is simply not obtainable by invasive biopsy procedures that not only just provide a limited histological “snapshot” but may also be harmful for the patient.

MRI cell tracking, with its superior spatial resolution and excellent soft tissue anatomical detail, is now emerging as the technique of choice to monitor in real-time image-guided cell delivery and engraftment. Up until now, 10 clinical MRI cell tracking studies have been published, either using superparamagnetic iron oxide nanoparticles (SPIO) for proton (1H) or perfluorocarbons for fluorine (19F) MRI. SPIOs create strong local magnetic field disturbances that spoil the MR signal leading to hypointense contrast, while the fluorinated compounds generate signal “hot spots” similar as those seen in nuclear medicine studies.

Twelve years ago, our Cellular Imaging Section in the Johns Hopkins Institute for Cell Engineering was part of the team that performed the first-in-man 1H MRI SPIO-labeled cell tracking study. Previous imaging studies used 111In-oxine (radio) labeled cells and ultra-sound guided local tissue injection. A major surprise, and only revealed by MRI, was that the cells missed their target in half the patients. Our second clinical 1H MRI SPIO-labeled stem cell tracking study in patients with amyotrophic lateral sclerosis (ALS) and multiple sclerosis (MS) showed that systemically and intrathecally injected mesenchymal stem cells (MSCs) homed into neuroinflammatory lesions in the brain and spinal cord, where they act as immunomodulators. We recently obtained IND approval for a first-in man trial on 19F MRI of perfluorocarbon-labeled stromal vascular fraction (SVF) cells for treatment of radiation-induced fibrosis in women with breast cancer. We will be scanning the first patients by the end of this year (NCT02035085).

## Lightweight Technology for Interventional Medicine: An Optical Flow Approach to Tracking Colonoscopy Video

**Terry S. Yoo**

*School of Computing and Information Science, University of Maine, Orono, ME, USA*

### Abstract

There is a natural marriage in radiology between computing and medicine. As radiology has diversified from diagnosis to treatment and intervention, the trend has been to make a substantial investment in technology and infrastructure leading to interventional suites, navigational tracking systems, and workstations for surgical guidance. At the same time, computers have become smaller, more powerful, more pervasive, and yet less physically intrusive in our daily lives. A theme in my research has been to investigate approaches that leverage this increase in computing power while reducing the footprint of technology in our procedures, seeking lightweight technological solutions for interventional medicine.

This work is a proof of concept showing that we can supplement the clinical value of an optical colonoscopy procedure if we can continuously co-align corresponding virtual colonoscopy (from a preoperative X-ray CT exam) and optical colonoscopy images. When presented with a pre-operative virtual colonoscopy based on an X-ray CT scan of the patient, our research has shown that we can track the position of the colonoscope along the colon using dead reckoning and velocity derived from optical flow characteristics of the endoscopic video. We have introduced new computer vision techniques of region flow and temporal volume flow to increase the stability of our video-based tracking and to aid in position recovery after the endoscope is obscured.

Our work was developed using public repositories of colonoscopy case studies, emphasizing the need to increase and improve the availability of open data in our community.

## Advances in Intraoperative Imaging and Registration for Image-Guided Interventions

**Jeffrey H. Siewerdsen**

*Department of Biomedical Engineering, Johns Hopkins University, Baltimore, MD, USA*

### Abstract

Emerging methods and technologies permit improved 3D image quality and reduced radiation dose in image-guided interventions in support of high-precision targeting, avoidance of collateral normal anatomy, as well as decision support and safety checks. Similarly, the ability to deformably register multiple sources of preoperative and intraoperative imaging offer enhanced visualization and a basis for quality assurance of the surgical product with respect to preoperative planning. Such

capabilities offer to extend the utility of imaging and registration from a relatively narrow scope of procedures requiring high precision to a broader scope that benefit more generally from Operating Room Quality Assurance (ORQA). They also point to emerging, data-intensive approaches to patient-specific planning and better understanding of factors governing variability in treatment outcome.

## Machine Learning + Knowledge Modeling: Medical Image Recognition, Segmentation and Parsing

S. Kevin Zhou

*Institute of Computing Technology, Chinese Academy of Sciences, China*

### Abstract

The “Machine learning + Knowledge modeling” approaches, which combine machine learning with domain knowledge, enable us to achieve start-of-the-art performances for many tasks of medical image recognition, segmentation and parsing. In this talk, we first present real success stories of such approaches. Then, we review the latest about deep learning. Finally, we demonstrate that the knowledge-fused deep learning approaches enable an extra performance boost.

### Featured Presentations

## Correction of Grade 2 Spondylolisthesis Following a Non-Surgical Structural Spinal Rehabilitation Protocol Using Lumbar Traction: A Case Study and Selective Review of Literature

Curtis Fedorchuk

*Certified – Chiropractic Biophysics, Better Health by Design, Cumming, GA, USA*

### Abstract

**Objective:** Discuss the use of non-surgical spinal rehabilitation protocol in the case of a 69-year-old female with a grade 2 spondylolisthesis. A selective literature review and discussion are provided.

**Clinical Features:** A 69-year-old female presented with moderate low back pain (7/10 pain) and severe leg cramping (7/10 pain). Initial lateral lumbar X-ray revealed a grade 2 spondylolisthesis at L4-L5 measuring 13.3 mm.

**Interventions and Outcomes:** The patient completed 60 sessions of Mirror Image<sup>®</sup> spinal exercises, adjustments, and traction over 45 weeks. Post-treatment lateral lumbar X-ray showed a decrease in translation of L4-L5 from 13.3 mm to 2.4 mm, within normal limits. 18 Month follow up shows continued stability of the segment despite two automobile car crashes.

**Conclusions:** This case provides the first documented evidence of a non-surgical or chiropractic treatment, specifically Chiropractic BioPhysics<sup>®</sup>, protocols of lumbar spondylolisthesis where spinal alignment was corrected. Additional research is needed to investigate the clinical implications and treatment methods.

## Lenticulostriate Vasculopathy in Preterm Infants: A New Classification, Clinical Associations and Neurodevelopmental Outcome

Julide Sisman

*UT Southwestern Medical Center, Department of Pediatrics, Division of Neonatal-Perinatal Medicine, Dallas, TX, USA*

### Abstract

Lenticulostriate vasculopathy (LSV) is a sonographic term given to “branching hyperechogenic lines” in the basal ganglia and/or thalamus seen on cranial ultrasound scans. LSV was first described on a neonatal cranial ultrasound in 1985, but the clinical importance, relevance to congenital infections, and long-term consequences of LSV on neonatal cranial ultrasound continues to be unclear. The incidence of LSV being reported has increased recently, which might reflect nothing more than a

growing awareness of this finding on neonatal cranial ultrasound. On the other hand, improved ultrasound imaging technology may have enhanced identification, and there may be an increase in the frequency of risk factors contributing to the presence of LSV. We suspect that improvements in US technology have enhanced the visibility of the arterial walls in the supratentorial deep gray matter. Thus, thin and faint lenticulostriate vessels that are seen on neonatal cranial US using contemporary technology may not necessarily be pathological.

This presentation on LSV provides an update of current knowledge, with emphasis on definition and challenges that might have evolved with establishing the diagnosis during the last three decades. It has been accepted that lenticulostriate arteries supplying the deep gray matter are not normally visualized on the cranial ultrasound. For the first time in the literature, we challenged this notion in light of the recent technological advances in ultrasound imaging that have enhanced ultrasound imaging. Conflict still exists in terms of the clinical importance and long-term outcomes of LSV since the first case reported three decades ago. In this article, we also scrutinized the available evidence on clinical correlation of this neonatal ultrasound finding, discussed long-term outcomes, and provided strategies that may guide practitioners in clinical settings.

## The Role of Arteriolar Blood Vessels for Preclinical Stages of Neurodegenerative & Chronic Psychiatric Diseases

Jun Hua

Kennedy Krieger Institute, Johns Hopkins University School of Medicine, Baltimore, MD, USA

### Abstract

The arterioles are the most actively regulated blood vessels, and thus may be more sensitive to metabolic disturbances in the brain. Using advanced MRI techniques (iVASO MRI) at 7T, we investigate abnormalities in the volume of small pial arteries and arterioles (CBVa) in brain diseases. In Alzheimer's disease, we found significantly elevated CBVa in MCI subjects compared to cognitively normal controls. Interestingly, many regions with elevated CBVa in MCI overlapped with regions showing increased A $\beta$ -deposition in PiB PET scans. In Huntington's disease, we found significantly elevated CBVa in the frontal cortex which correlated with the projected year-to-onset of motor symptoms in patients. In Schizophrenia, significant CBVa reduction was detected in multiple brain areas, which correlated with disease duration. The fact that opposite changes in CBVa were measured in different diseases suggests that the abnormalities observed are not likely due to undetected systemic bias or artifact.

## Clinical, Genetic, and Neuroimaging Characterization of Patients with Developmental and Iatrogenic Inter-Hemispheric Disconnection

Lana Vasung<sup>1</sup>, Claude Lepage<sup>2</sup>, Arthur Rezayev<sup>1</sup>, Jacob Levman<sup>1,3</sup>, Joseph Madsen<sup>4</sup>, Alan Evans<sup>2</sup> and Emi Takahashi<sup>1</sup>

<sup>1</sup>Division of Newborn Medicine, Boston Children's Hospital, Harvard Medical School, Boston, MA, USA

<sup>2</sup>McGill Centre for Integrative Neuroscience/Montreal Neurological Institute, McGill University, Canada

<sup>3</sup>Department of Mathematics, Statistics and Computer Science, St. Francis Xavier University, Canada

<sup>4</sup>Department of Neurosurgery, Boston Children's Hospital, Harvard Medical School, Boston, MA, USA

### Abstract

The goal of our work was to assess the effect of abnormal development of the corpus callosum (CC) or iatrogenic loss of callosal fibers on the microstructural/morphological development of the cerebral cortex and the patient's clinical outcomes. Data from patients with dysgenesis of the CC and patients that underwent a surgical removal of the cortex due to the epilepsy were retrieved from a Boston Children's Hospital MRI database. MRIs of patients with dysgenesis of the CC (N = 39, Group-1) and MRIs of patients with epilepsy that were taken before and after surgery (N = 15, Group-2) were processed using CIVET (<http://mcin-cnim.ca/technology/civet/>). Age and sex-matched control group was assembled (Control-1, mean age at MRI scan; 8.08  $\pm$  3.98 years).

Based on the appearance of the CC, Group-1 was divided into two sub-groups: hypoplasia (N = 21) and agenesis (N = 18). There was no significant difference between them in patient characteristics, presence of clinical, brain, genetic abnormalities, or in quantitative brain measures.

Group-1, compared to the control group, had significantly greater odds of having gene/chromosomal abnormality (Odds Ratio; OR = 9.2), bulbar (OR = 23.7), muscular tone (OR = 44.4), motor (OR = 7.5), language (OR = 67.9), behavioral disorder

(OR = 8.4), or epilepsy (OR = 23). Patients in Group-1, compared to controls, had significantly smaller white matter volumes, gyrification index (GI), cortical surface area, and the mean cortical thickness. Fractional anisotropy and apparent diffusion coefficient, microstructural correlates, of the cerebral cortex were not significantly different between patients with dysgenesis of CC and controls.

Majority of patients (98%) that underwent a surgical procedure (Group-2) did not show new clinical symptoms. Cortical surface area, mean cortical thickness, and GI of the healthy hemisphere were not statistically significantly different before and after the surgery (controlled for the time period between surgery and the last MRI).

Our results indicate importance of developmental timing of inter-hemispheric connectivity for proper structural/functional maturation of the cerebral cortex.

## MRI Diagnosis of Infantile Alexander Disease in a 14-Month-Old African Boy: A Case Report

Nondumiso Dlamini\* and Vicci du Plessis

*Nelson R. Mandela School of Medicine, University of KwaZulu-Natal, South Africa*

### Abstract

Alexander disease, also known as fibrinoid leukodystrophy, is a rare leukoencephalopathy which occurs due to a mutation in the glial fibrillary acid protein (GFAP) gene. Magnetic resonance imaging (MRI) has proven to be highly sensitive in making the diagnosis. Typical MRI findings, in combination with positive genetic blood analysis, confirm the diagnosis. Three subtypes have been described; that is, infantile, juvenile and adult types. We present a case of a 14-month-old boy who was diagnosed with Alexander disease based on MRI findings.

## Association of Childhood Obesity with the Central Nervous System: Study of Diffusion Tensor Imaging (DTI)

Pamela Bertolazzi<sup>1,2\*</sup>, Fabio L. S. Duran<sup>1</sup>, Cecilia Kochi<sup>3</sup>, Marília Seelaender<sup>3</sup>, Naomi Antunes<sup>1</sup>, Elie B. Calfat<sup>2</sup>, Thaysa Neves<sup>2</sup>, Pedro L. A. M. Souza<sup>2</sup> and Ricardo R. Uchida<sup>2</sup>

<sup>1</sup>Neuroimaging Laboratory, Psychiatric Department of University of Sao Paulo, Medical School, SP, Brazil

<sup>2</sup>Irmandade da Santa Casa of Sao Paulo, SP, Brazil

<sup>3</sup>Biomedical sciences Institute of University of Sao Paulo, SP, Brazil

### Abstract

**Background:** Previous studies have shown atrophy in gray matter and decrease of white matter (WM) connectivity in several brain regions of obese adults. However, there are controversial results about WM integrity of obese children and adolescents. Childhood obesity is an important healthy concern around the world, therefore, the aim of this study is to investigate the influence of childhood obesity on change in cerebral connectivity, using Diffusion Tensor Imaging (DTI) by Magnetic Resonance (MRI).

**Methods:** The images were obtained on 3T MRI scanner, and the sample consisted of 117 subjects, of which, 57 obese and 60 normal weight adolescents. The average of age was 13 years old and there were no significant statistical differences ( $p > 0.05$ ) between the groups in reference of gender, education, socioeconomical classification and sexual development, except for Body Mass Index (BMI, Z-score,  $p < 0.001$ ) as expected. The images process was performed using FSL and the fractional anisotropy (FA) values were compared between the above groups using Statistical Parametric Mapping from MATLAB.

**Results:** The analysis revealed that obese group had decrease of FA in WM regions, when compared to the control group, including the corpus callosum (splenium and body) and medium orbital gyrus. There were no higher FA values in obese group.

**Conclusions:** These findings suggest that obese adolescents may have demyelination in regions of the brain related to impulse control and cognitive functions.

## Dynamic MR Imaging (MR Fluoroscopy): Clinical Applications in Pediatric Neuroradiology

Tamara Feygin

University of Pennsylvania, Perelman School of Medicine, Philadelphia, PA, USA

### Abstract

Dynamic cine magnetic resonance imaging (MR “fluoroscopy”) is a rapidly developing technique, which evolves from research and works in progress into routine imaging sequences. This technique is designed to demonstrate some of the physiologic and pathologic processes of the human body in almost real time. MR “fluoroscopy” offers many advantages over other dynamic imaging modalities (such as X-ray-based fluoroscopy or nuclear medicine examinations) due to its lack of ionized radiation and short acquisition time. These features are particularly important in pediatric and prenatal medicine. The dynamic sequences are based on fast acquisition and organization of images in a sequential-loop, resulting in an impression of observing a real-time movie. The sequences vary slightly in different manufactures but almost any sequence sensitive to flow may be employed. They are easily obtainable from a technical standpoint and are easily tolerated by patients. These dynamic sequences prove to be valuable tools in functional assessment of intracranial/intraspinal CSF flow dynamics; evaluation of effectiveness of endoscopic procedures; evaluation of the phonation in children with suspected velo-pharyngeal dysfunction, sleep apnea, etc. and swallowing patterns in fetuses with head and neck lesions. Dynamic cine MR imaging improves our knowledge of fetal physiology and provides clinically significant prognostic information for pre and postnatal planning. A comprehensive review of dynamic MR techniques and examples of its utilization in pediatric neuroradiology will be demonstrated.

## Model-free Characterization of the Microstructure of the Living Human Brain with 5D Relaxation Diffusion Tensor Correlation MRI

J. P. de Almeida Martins<sup>1,2</sup>, C. M. W. Tax<sup>3</sup>, F. Szczepankiewicz<sup>1,2,4</sup>, M. Chamberland<sup>3</sup>, G. Eklund<sup>2</sup>, K. Bryshke<sup>2</sup>, D. K. Jones<sup>3</sup>, C. F. Westin<sup>4</sup> and D. Topgaard<sup>1</sup>

<sup>1</sup>Lund University, Sweden

<sup>2</sup>Random Walk Imaging AB, Sweden

<sup>3</sup>Cardiff University, United Kingdom

<sup>4</sup>Harvard Medical School, Boston, MA, USA

### Abstract

Conventional quantitative MRI yields voxel average relaxation rates and diffusion tensors that are difficult to interpret in terms of chemical composition and microstructure whenever the voxels contain more than one tissue type such as white matter (WM), gray matter (GM), and cerebrospinal fluid (CSF). Here, we propose a protocol to quantify per-voxel heterogeneity as 5D joint relaxation diffusion tensor relaxations. A healthy volunteer was scanned with a diffusion-weighted EPI sequence customized for variable echo times and tensor valued diffusion encoding. The used 5D acquisition protocol establishes correlations across the dimensions of the distributions, namely: the transverse relaxation rate R2, isotropic diffusivity, normalized diffusion anisotropy, and diffusion tensor orientation (two dimensions). The acquired data yields the sought-for distributions upon unconstrained Monte Carlo inversion. Voxels containing pure WM, GM, or CSF give nearly single mode distributions (WM: high R2, low diffusivity, high anisotropy; GM: high R2, low diffusivity, low anisotropy; CSF: low R2, high diffusivity, low anisotropy), while voxels with binary mixtures yield the corresponding bimodal distributions. Component resolved maps of signal amplitude, R2, diffusivity, anisotropy, and orientation for the WM, GM, and CSF fractions are obtained by binning and parameter calculation in the 5D distribution space.

Our image acquisition protocol and model free data inversion procedure yields per-voxel quantification of distinct tissue types without relying on assumptions about the number or properties of the individual components. The new method is expected to be useful for pathological conditions associated with sub-voxel tissue heterogeneity such as tumor infiltration in surrounding brain tissue.

## De Novo Formation of Spinal Pial Arteriovenous Fistula Ten Years Post-Resection of Different AVFs

Tahaamin Shokuhfar<sup>1</sup>, Michael Hurley<sup>1</sup>, Sameer Ansari<sup>1</sup>, Matthew Potts<sup>2</sup>, Babak Jahromi<sup>2</sup> and Ali Shaibani<sup>1</sup>

<sup>1</sup>Department of Radiology, Feinberg School of Medicine, Northwestern University, Chicago, IL, USA

<sup>2</sup>Department of Neurological Surgery, Feinberg School of Medicine, Northwestern University, Chicago, IL, USA

### Abstract

Although pial AVFs were considered as a subtype of arteriovenous malformation (AVM), currently they are categorized separately due to their distinct pathology, clinical course and therapeutic approaches. The pathogenesis of pial AVF is not fully understood but aberrations in the formation of the capillary network during embryogenesis are thought to have a significant role in its development. Syndromes like hereditary hemorrhagic telangiectasia (HHT) and Klippel-Trenunay-Weber (KTW) have been shown to be associated with spinal pial AVFs as well. Different classifications have been introduced for spinal arteriovenous shunts (AVS), the most common one classifying spinal AVS into four groups: type I (Dural AVF), type II (glomus AVM), type III: juvenile metamer AVM and type IV: spinal pial AVF. Traditionally, spinal pial AVFs are always considered congenital malformations causing symptoms in early childhood or later in adulthood. Here, we are presenting a patient with new spinal pial AVFs 10 years after resection of 3 pial AVFs which were more cranially located. Her initial symptoms began with right side lateral foot and posterior thigh progressive pain later were associated with 3 spinal pial arteriovenous fistulas (AVF) in 2004. She subsequently underwent endovascular treatment and T11 to L1 laminectomy with resection of AVFs in 2005, with a postoperative angiogram demonstrating no residual malformation. Ten years later, she presented with new right lower extremity weakness, perineal pain, and new left plantar foot numbness. Repeat spinal angiography demonstrated two intertwined conus medullaris AVMs. To the best of our knowledge, there are no reports of de novo formation of spinal pial AVFs after the complete cure of the initial lesion in English literatures.

## Optical Imaging of Dose for Comprehensive Quality Assurance in Radiation Oncology

Petr Bruza<sup>1</sup>, David Gladstone<sup>2,3</sup>, Lesley Jarvis<sup>2,3</sup> and Brian Pogue<sup>1,2</sup>

<sup>1</sup>Thayer School of Engineering, Dartmouth College, Hanover, NH, USA

<sup>2</sup>Geisel School of Medicine, Dartmouth College, Lebanon, NH, USA

<sup>3</sup>Norris Cotton Cancer Center, Lebanon, NH, USA

### Abstract

Clinical dose deposition into tissue or water is always accompanied by a light emission through Cherenkov and/or scintillation mechanisms. In principle, the optical emission surrogates the dose. High resolution and high frame rate imaging of this optical emission can therefore provide novel solutions for rapid quality assurance (QA) of radiotherapeutic beam delivery. The first part of this presentation is dedicated to imaging and real-time 3D reconstruction of dose volume to liquid phantoms. It has been previously demonstrated that optical imaging dosimetry offers a robust, accurate, and efficient method for machine and end-to-end QA for standard C-arm systems, as well as for MRI guided radiotherapy devices. The second part will provide insights into a novel in vivo Cherenkov imaging system, capable of imaging surface dose on patients in real time. Comparing the recorded Cherenkov images with the treatment plan will seamlessly inform clinicians about fraction-to-fraction changes of beam geometry with respect to patient's anatomy.

## 68 Ga - PSMA, Initial Experience and Future Applications

Felipe Roth Vargas<sup>1</sup>, Douglas Jorge Raci, Leticia Rigo and Roberta Morgado Zuppani

<sup>1</sup>BP Medical Center, São Paulo, Brazil

### Abstract

Prostate cancer diagnostic has a well established protocol regarding imaging, metabolic and biopsy, but there are still some gaps to be filled regarding metabolic recurrence, especially in cases after radical prostatectomy without primary focus.

Metabolic evaluation with FDG-PET/CT, computed tomography and full body magnetic resonance has its role whenever patients with elevated PSA from obscure origin need a research for local recurrence and metastatic distant sites, the applications

of 68 Ga-PSMA ligand has shown promising results for detection of suspicious malignant sites, making early target treatment more effective and resulting in better outcomes.

For the establishment and rational application of this modality is fundamental to understand the physiological distribution before concerning yourself with pathological signs, the objective of this project is to illustrate our initial experience and future the expectation for this radio tracer in prostate cancer diagnosis and treatment.

## Comparison of Clinical and Phantom Image Quality for Low Contrast Liver Lesion in a Prospective Multicenter CT Scanner Dose Optimization Program

Hugues Brat<sup>1</sup>, Damien Racine<sup>2</sup>, Stephane Montandon<sup>3</sup>, Benoit Rizk<sup>4</sup>, Dominique Fournier<sup>1</sup> and Federica Zanca<sup>5</sup>

<sup>1</sup>Institute of Radiology of Sion, Groupe3R, Switzerland

<sup>2</sup>Institute of Radiation Physics, Lausanne University Hospital, Switzerland

<sup>3</sup>Philips Healthcare, The Netherlands

<sup>4</sup>Fribourg Medical Imaging Center, Groupe3R, Switzerland

<sup>5</sup>GE Healthcare, France

### Abstract

**Purpose:** To compare diagnostic performance for low contrast liver lesions on patient and phantom images in a prospective multicenter CT scanner dose optimization study.

**Methods and Materials:** A protocol optimization study based on clinical indication and BMI with stepwise dose reduction was implemented on 5 CT scanners (Philips™). 3035 abdomen CT examinations were prospectively assessed for diagnostic image quality (visual assessment and European guidelines). A subgroup of 33 patients who underwent a liver examination (tumor or cancer staging) were evaluated for image quality before and after optimization. In parallel, phantom (QRM™ 401 abdomen) acquisition with 2.5 (size M) and 5 cm (size L) fat ring was performed before and after dose optimization using the same liver tumor follow-up protocol. A Channelized Hotelling (CHO) model observer was used to assess lesion detectability in phantom images, using the ROC paradigm with the area under the ROC curve (AUC) as figure of merit.

**Results:** Median patient CTDI<sub>vol</sub> value decreased from 6.8 to 5.2 mGy (-24%) and from 10.8 to 8.5 mGy (-22%) respectively for BMI < 25 and > 25 patients. For phantom images, mean CTDI<sub>vol</sub> value decreased from 8.8 to 6.3 mGy (-28%) for M-sized and from 15.9 to 11.8 mGy (-26%) for L-sized phantom. No non-diagnostic votes were registered in the 33 paired patients' subgroup. Phantom images analysis showed constant low contrast lesion detectability until 26% dose reduction. However, additional dose reduction impaired detectability of 5 mm lesions.

**Conclusion:** Combining clinical and phantom diagnostic image quality enabled dose reduction according to the ALARA principle without impairing low contrast liver lesion detectability.

## Diffusion Tensor Imaging and Fibre Tracking Biomarkers of Intramedullary Tumours of Spinal Cord for Predictive Resectability Scoring-Observational Comparative Study of 48 Cases

Ram Mohan Vadapalli<sup>1</sup>, Vijaya Saradhi Mudumba<sup>2</sup> and A. S. Vadapalli<sup>3</sup>

<sup>1</sup>Consultant Radiologist, Vijaya Diagnostics, Hyderabad, India

<sup>2</sup>Nizam's Institute of Medical Sciences, Hyderabad, India

<sup>3</sup>Armed Forces Medical College, Pune, India

### Abstract

**Purpose:** The aim of this prospective observational comparative study is to evaluate the role of diffusion tensor imaging (DTI) in management of intramedullary spinal cord lesions (IMSCl) for predicting "safe resectability" to assess subsequent outcomes.

**Methods and Materials:** DTI was performed in 65 patients with IMSCl (intramedullary spinal cord lesions) and contrast enhanced MRI. 38 males, 27 females; mean age of 37.5 years was recruited in the study. Medium resolution DTI (diffusion Tensor Imaging) on a 3T MRI (Philips Ingenia scanner) with Axial Plane; b values: 0, 1000; Number of directions 15. Tumour matrix fractional anisotropy (FA), tumour cord interface FA and tractograms were assessed, correlated with intraoperative

findings and neurological outcomes after surgery.

**Results:** There were 65 patients (38 males, 27 females; mean age of 37.5 years) in this study, 50 were neoplastic (19 ependymomas, 14 astrocytoma's, 3 metastases, 4 hemangioblastoma, 5 cavernomas, 5 lipomas); 15 were non-neoplastic - DTI was used to classify the lesions as completely resectable (18), partially resectable (26) un-resectable (6). 2 patients lost for follow up: Not included in analysis. Spearman's Correlation coefficient between DTI prediction of cleavage plane and intra operative finding of plane was 0.84 ( $p$  value < 0.001). All the patients where DTI concluded the lesion is resectable had a good outcome (61.1% vs 0.0%;  $p$  < 0.001); significantly higher number of patients had poor outcome if DTI concluded the lesion was not resectable (19.4% vs 66.7%;  $p$  = 0.015).

**Conclusion:** This study suggests that DTI is useful in predicting the safe resectability of IMSCL.

## Pictorial Review of Extra-Osseous Ewing's Tumour, A Single Center Experience in Pakistan

Muhammad Bilal Fayyaz\*, Imran Khalid Niazi and Amjad Iqbal

Radiology Department, Shaukat Khanum Cancer Hospital & Research Centre, Pakistan

### Abstract

**Purpose:** Ewing's Family tumour is an extremely rare tumour, with annual incidence rates among Caucasian children less than 21 years being in the range of 2-3 cases per million in the U.S. There are mainly three subtypes including Ewing's sarcoma of bone, extraosseous Ewing's tumour and peripheral primitive neuroectodermal tumour (PPNET). Although extremely rare, this study represents a review of various types of cases and the significance of imaging including its baseline and post treatment response radiological characteristics. There are a very few cases of extraosseous Ewing's sarcoma in current literature with variable spectrum of tumour site and there imaging characteristics.

**Material and Methods:** Electronic records were retrospectively reviewed from 01-05-2011 to 01-05-2016 with patients who were diagnosed as histologically proven Ewing's sarcoma. Number of patients, gender and baseline CT/MRI findings for staging were reviewed.

**Results:** A total of 568 patients with diagnosed Ewing's Sarcoma were analyzed out of which 15 patients had extraosseous type of Ewing's Sarcoma. Out of which only 8 patients had baseline imaging available including tumours arising from occipital region, orbit, anterior mediastinum, anterior abdominal wall, mesentery, kidney, prostate gland and pre-sacral region.

**Conclusion:** Extraosseous Ewing's sarcoma is a rare entity and can involve a wide array of soft tissue organs. Cross sectional imaging with CT and MR has a key role in pre and post treatment assessment.

## PET-CT with 18F-FDG Labeled Leucocytes - A New Paradigm in Infection Imaging

Anish Bhattacharya

Department of Nuclear Medicine, Postgraduate Institute of Medical Education and Research, Chandigarh, India

### Abstract

Early and accurate detection of infection is important to initiate effective treatment. Laboratory investigations like erythrocyte sedimentation rate and C-reactive protein estimation are non-specific and sampling of the suspected tissue with pathological/microbiological confirmation remains the gold standard for diagnosis. However, inaccessibility of the organ of interest or adverse patient situations may necessitate less invasive methods of diagnosis. Ultrasonography and computed tomography provide excellent spatial resolution but lack functional specificity. In-111 and Tc99m labeled leucocyte scintigraphy, the standard infection imaging techniques, have inferior spatial resolution.

We have developed a simple technique for infection imaging using positron emission tomography/computed tomography (PET-CT) with 18F-Fluorodeoxyglucose (FDG) labeled autologous leucocytes (separated from 40 ml of the patient's venous blood). PET-CT imaging two hours after tracer injection (compared to 24 hours for Tc99m/In-111 labeled leucocytes) provides superior image quality with no adverse effects in any patient during/after the procedure. Physiological tracer distribution is limited to the liver, spleen and bone marrow, with minor clearance of unlabeled FDG through the kidneys and bladder. This safe, non-invasive and cost-effective technique accurately identifies and localizes infection at an early stage. We have found it useful in imaging infected peri-pancreatic collections in acute pancreatitis as well as infections in bones, joints, cardiac valves, pacemaker leads, skull base osteomyelitis and diabetic foot osteomyelitis in the setting of Charcot's arthropathy. Important

limitations are that the time-consuming leucocyte labeling procedure involves handling of patients' blood, requires meticulous aseptic technique and requires a dedicated laboratory with trained staff.

## Radiologist-Centered Artificial Intelligence for Lung Cancer Diagnosis

Ulas Bagci

*Center for Research in Computer Vision (CRCV), University of Central Florida, Orlando, FL, USA*

### Abstract

Lung cancer screening with low dose computed tomography (CT) was shown to reduce lung cancer mortality by 20%. Yet, human error remains a significant problem to detect abnormalities. To alleviate some of these diagnostic errors (such as missing tumors and misdiagnosis), computer aided diagnosis (CAD) tools have been developed to help radiologists. However, conventional CADs have serious limitations such as a large number of false positive findings and high execution times. Radiologists are expected to eliminate false positive findings generated by the CAD systems, which makes majority of CADs infeasible in routine practice. Furthermore, conventional CAD systems could not go beyond being second opinion tools. In this study, I aim to show strategies for develop a paradigm shifting CAD system, called collaborative CAD (C-CAD), that creates a communication channel with radiologists and create a true collaboration with them for a more accurate and efficient CAD system, called "radiologist-centered artificial intelligence (AI) for lung cancer diagnosis". We use eye-tracking systems in realistic radiology room settings, and more recent AI techniques, namely deep learning, to combine strengths of radiologists and AI based interpretations for lung cancer diagnosis. Promising results support the efficiency, accuracy, and applicability of the proposed CAD system in a real radiology room setting.

## Retrospective Study of Diagnostic Performance of 18F-FDG PET-CT in Cases Referred as Carcinoma of Unknown Primary

Priya A, Pradeep, Venugopal M, Ramachandran and Minolin Dhas

*Regional Cancer Centre, Trivandrum, Kerala, India*

### Abstract

**Aim:** To estimate the clinical effectiveness of fluorodeoxyglucose (FDG) Positron emission tomography-computed tomography (PET-CT) in detecting the primary tumor in cases referred as CUP and identifying a group of patients, who are likely to be benefitted with FDG PET-CT.

**Methods:** 65 CUP patients who underwent PET-CT from January 2016-April 2018 whose imaging and clinical data were available in PACS and hospital records were included. This comprises patients referred for PET-CT as an initial investigation, patients referred after an extensive conventional work up failed to detect a primary site and patients whose initial PET CT was negative for primary mass detection and were reassessed with PET-CT for treatment response after empirical chemotherapy. In most of the cases, histopathological proof was taken as reference standard for metastasis. In cases where biopsy was not feasible (n = 11) like brain metastasis, pulsatile bone lesions, choroidal lesions of the eye, imaging and other relevant diagnostic investigations were also accepted as reference standard.

**Conclusion:** In cases where PET-CT was diagnostic of primary tumour, conventional CT also detected the primary and hence found beneficial only in staging. PET- CT could not detect the primary site in all 40 patients, who were negative on conventional imaging work up. Of these 8 were false negative on subsequent work up. PET-CT was beneficial in patients sent for response assessment after empirical treatment. In lesions where histopathology was not feasible, it helped in ruling out other lesions and narrowing down diagnosis.

## Novel Preclinical PET/CT Tracers for the Evaluation of Sarcomas

Ronnie A. Sebro\* and Ian Sigal

*Department of Radiology, University of Pennsylvania, Philadelphia, PA, USA*

### Abstract

Sarcomas are rare heterogeneous tumors of mesenchymal origin with poor prognosis. New imaging positron emission

tomography (PET) tracers now provide the unique opportunity to evaluate sarcoma growth, metabolism, and sarcoma tumor biology. This talk will focus on sarcoma biology, focusing on glucose metabolism/glycolysis, hypoxia, proliferation and protein synthesis. Novel pre-clinical imaging PET tracers will be discussed, highlighting particular strengths and limitations of each novel PET tracer and clinical findings reported in the literature. Particular emphasis is placed on the role that these new tracers can play in our understanding of sarcomas.

## Texture Analysis of Apparent Diffusion Coefficient Maps to Differentiate Between High-grade Gliomas and Metastatic Brain Tumors

Padikkalakandy Cheriya Shesnia Salim\*, Brayin Pokkantakath Rishal Reshin and Yan-Wei Miao

Dalian Medical University, China

### Abstract

**Purpose:** To evaluate the diagnostic ability of Texture Analysis of Apparent Diffusion Coefficient (ADC) maps to differentiate between High-grade gliomas (HGG) and Metastatic brain tumors (METS).

**Methods and Materials:** ADC maps of intra-tumoral and peri-tumoral regions of the Diffusion Weighted Images of 50 patients with HGG and 32 patients with METS were recorded using ADW 4.6 workstation Functool2 software. With Omni kinetics software, texture parameters including MIN, MAX, MI, skewness, kurtosis, MD, RD, VVS, RMS, uniformity, VC, energy, entropy, correlation, IDM, CP, GLN, RLN, LGLRE, HGLRE, SRLGLE, SRHGLE, LRLGLE and LRHGLE of the 3D merged Region of Interests images were recorded. Shapiro-Wilk test for normality and independent sample t-test (parametric) and Mann-Whitney U test (non-parametric) were carried out (spss 20.0). ROC curve tests were performed to calculate AUC, cutoff values, sensitivity and specificity.

**Results:** 1) VC ( $p = 0.009$ ), VVS ( $p = 0.013$ ), RMS ( $p = 0.000$ ), RD ( $p = 0.042$ ), correlation ( $p = 0.016$ ), energy ( $p = 0.000$ ), entropy ( $p = 0.000$ ), GLN ( $p = 0.009$ ), RLN ( $p = 0.005$ ), LGLRE ( $p = 0.023$ ), SRLGLE ( $p = 0.027$ ), LRLGLE ( $p = 0.000$ ) and LRHGLE ( $p = 0.030$ ) between HGG and METS are statistically significant. 2) ROC curve analysis showed good differentiating diagnostic ability for HGG and METS with regards to entropy (AUC = 0.955), RLN (AUC = 0.684), VC (AUC = 0.672), GLN (AUC = 0.671), VVS (AUC = 0.663), correlation (AUC = 0.659) and RD (AUC = 0.634). Entropy showed the highest AUC (0.955), sensitivity (91.8%) and specificity (100%).

**Conclusion:** Texture Analysis of quantitative ADC maps based on entire region of tumor serve as good differentiating diagnostic indices of HGG and METS.

## Unified Heat Kernel Regression for Diffusion, Kernel Smoothing and Wavelets on Irregular Image Domains and Its Application to Lung Blood Vessel Trees

Moo K. Chung<sup>1\*</sup> and Gurong Wu<sup>2</sup>

<sup>1</sup>Department of Biostatistics & Medical Informatics, University of Wisconsin-Madison, Madison, WI, USA

<sup>2</sup>University of North Carolina at Chapel Hill, NC, USA

### Abstract

We present a unified kernel regression framework for smoothing data using the Laplace-Beltrami eigenfunctions. Starting with the heat kernel constructed from the eigenfunctions, we formulate a new bivariate kernel regression framework as a weighted eigenfunction expansion with the heat kernel as the weights. The new kernel method is mathematically related to isotropic heat diffusion, kernel smoothing and diffusion wavelets. Various mathematical and statistical properties useful for medical imaging applications will be presented. As an application, we show how to obtain the skeleton representation of the human lung blood vessel trees from CT. The skeleton representation is further used in characterizing the topology of lung blood vessel trees.

## Medical Image Fusion and Augmented Reality

Raj Shekhar

Children's National Health System, Washington, DC, USA

## Abstract

An increasing trend in modern medicine is to collect and use images from multiple modalities for both diagnosing and treating diseases. Multimodality image fusion is particularly important in image-guided interventions (IGIs) in which the imaging modality used to guide the intervention may not provide an adequate visualization of the anatomy and/or the pathology. An example of this limitation is commonly seen in the percutaneous CT-guided interventional procedures where the targeted lesion may only be visible by PET or MRI but not by CT. Likewise, internal anatomical structures (vasculature, bile ducts, tumor, etc.) are not visualized in the real-time video of the surgical anatomy during laparoscopic procedures. And in image-guided radiotherapies, the treatment room cone-beam CT does not visualize the anatomy well enough to permit many advanced functions. A solution to this limitation is multimodality image guidance, in which pre and intra-interventional images merged by one of many techniques such as spatial tracking and automatic image registration. Efficient visualization of the guiding modality is also a prevailing limitation that modern head-mounted displays could potentially address. This presentation will cover some of the techniques that implement multimodality image guidance and a sampling of emerging applications.

## Optimizing the Optoelectronics for Retinal Polarization-Sensitive Scanning When Used in Combination with Other Ophthalmic Diagnostic Technologies

**Boris Gramatikov**

*Wilmer Ophthalmological Institute, Johns Hopkins University School of Medicine, Baltimore, MD, USA*

## Abstract

Retinal birefringence scanning has been recently used to detect central fixation and proper eye alignment in ophthalmic diagnostics. It utilizes the property of the retina surrounding the fovea (the most sensitive part of the retina) to change the polarization state of light in a double-pass polarization-sensitive optical system. This principle has been employed in a series of vision screeners developed in our lab. The usage can be expanded to add a fixation detection function to other ophthalmic technologies, such as laser-doppler flowmetry, fundus cameras, optical coherence tomography devices, etc. Although such a combination may appear straightforward, it poses a series of challenges. These include separating the two systems spectrally (to avoid interference with each other), presenting a visual target by means of a small LED or a computer-controllable LCD screen, communication between the two systems in real time, precise alignment, simultaneous aiming of the two systems, etc. Particularly important is the fact that most optical components in the combined path can also affect the polarization state of light, as does the human cornea. To address this issue, a computer model was developed that can be used to optimize system performance, i.e. maximize the signal while keeping the noise low. As an example, a hybrid system integrating optical coherence tomography and retinal birefringence scanning is presented. It acquires and/or analyzes data only during moments of central fixation. This can significantly reduce the image processing time and shorten the exam duration. Methods to attract the subject's attention are also discussed.

## The Benefit of Incorporating Ultrasound Imaging as Adjunct Teaching Tools to Enhance Physical Therapist Students' Ability and Confidence to Perform Manual Therapy

**Alycia Markowski, Maureen Watkins and Leslie Day**

*Northeastern University, Boston, MA, USA*

## Abstract

Historically, physical therapy (PT) students have struggled with their skill and confidence when performing manual techniques for musculoskeletal examination. To perform manual skills students, need to be comfortable with palpation skills, evaluating motor control and applying appropriate forces to stress tissues. Current teaching methods lack objective visual and kinetic feedback. Real-time ultrasound imaging (RTUI) provides objective concurrent visual feedback of anatomical structures and in-vivo joint changes.

Three different studies have evaluated the use of RTUI as an adjunct teaching tool for PT students.

The first study examined the use of RTUI for teaching and evaluating the accuracy of palpations of the medial collateral ligament of the knee. The second study focused on the ability to palpate and differentiate muscle contractions to identify motor control deficits of trunk musculature. The third study evaluated the use of RTUI as an adjunct teaching method to improve student's confidence and ability to perform manual knee traction. The use of RTUI during laboratory teaching improved

students' learning and accuracy in palpation of knee ligaments as well as students ability to identify change in deep muscle activation patterns. The use of RTUI for teaching manual knee traction showed positive trends toward improving student confidence scores and improving effectiveness of traction. RTUI appears to be an effective adjunct teaching method when combined with traditional teaching methods to include lecture and lab.

## **Precision Imaging- Better Image Quality for Focal Liver Lesions**

**Cisel Yazgan**

*Consultant Radiologist & Assistant Professor, Hacettepe University Faculty of Medicine, Turkey*

### **Abstract**

Sonography is usually the initial diagnostic modality in the evaluation of patients with suspected liver lesions. However, some image artifacts limit diagnostic accuracy of sonography. Hence, various new technologies have been developed to improve the diagnostic value of this modality.

Precision Imaging, a speckle reduction algorithm, improves signal noise ratio and provides higher image quality. In addition, it clearly shows contrast boundaries between tissues and lesions. The technique may be used as a complementary method in the sonographic evaluation of focal liver lesions.

## **Novel Method to Improve Radiologist Agreement in Interpretation of Serial Chest Radiographs in the ICU**

**D. A. Soboleski\*, D. Castro, M. Flavin, D. Manson and J. Flood**

*Queens University, Canada*

### **Abstract**

Several studies have documented poor intra and inter-observer agreement in the interpretation of imaging studies particularly in the ICU/NICU settings. Numerous factors can play a role in patient image acquisition, image quality and image analysis which can contribute to poor or erroneous perception of the radiographic findings and decrease our ability to provide consistency and reliable radiographic interpretations. The goal of this talk is to illustrate the role of our perception/perceptual skills in interpretation of imaging studies and to introduce novel methods including use of a Variable Attenuation Plate and associated software which may result in increased perception ability and help improve consistency in our interpretations of these cases. Two research ethic board approved studies recently published will be discussed which demonstrate a significant improvement in consistency of reporting of ICU and NICU chest radiographs when these methods are utilized. A third research ethic board approved sonographic study to illustrate the potential limiting role of an inherent perception ability on radiologic image interpretation will also be presented. Potential effects on patient care, hospital costs and possible solutions will be briefly discussed.

## **Morphologic Image Processing for Detection of Micro-Aneurysms in Fundus Images as Pre-Diagnosis of Diabetic Retinopathy**

**Roberto Rosas Romero**

*Department of Electrical and Computer Engineering, Universidad de las Américas, Mexico*

### **Abstract**

Diabetes increases the risk of developing any deterioration in the blood vessels that supply the retina, an ailment known as Diabetic Retinopathy (DR). It can only be diagnosed by an ophthalmologist. However, the growth of the number of ophthalmologists is lower than the growth of the population with diabetes so that preventive and early diagnosis is difficult. Preliminary, affordable and accessible ophthalmological diagnosis will give the opportunity to perform routine preventive examinations, during a stage of non-proliferation. During this stage, there is a lesion on the retina known as Micro-Aneurysm (MA), which is one of the first clinically observable lesions. In recent years, different image processing algorithms, for detection of the DR, have been developed; however, the issue is still open since acceptable levels of sensitivity and specificity have yet to

be reached. A different approach for MA detection is proposed which achieves sensitivity, specificity and precision of 92.32%, 93.87% and 95.93% for the diaretDB1 database.

## Radiomics-based Classification of the Phenotype of Pancreas Neoplasms

Seyoun Park<sup>1</sup>, Linda Chu<sup>1</sup>, Satomi Kwamoto<sup>1</sup>, Alan L. Yuille<sup>2,3</sup> and Elliot K. Fishman<sup>1</sup>

<sup>1</sup>Radiology and Radiological Science, Johns Hopkins University, Baltimore, MD, USA

<sup>2</sup>Cognitive Science, Johns Hopkins University, Baltimore, MD, USA

<sup>3</sup>Computer Science, Johns Hopkins University, Baltimore, MD, USA

### Abstract

Pancreatic Adenocarcinoma (PDAC) is one of the leading causes of cancer related death, and pancreatic cystic masses are detected in > 2% of abdominal CTs, and they vary in malignant potential based on underlying pathologic diagnosis. The purpose of this study is to determine if quantitative radiomics features can be used to differentiate pancreatic neoplasms from normal controls. IRB-approved 190 cases of pathologically proven PDAC, 103 cases with cystic mass, and 190 normal controls were retrospectively selected from the radiology and pathology databases. The whole pancreas boundary (including tumor region) were manually segmented from preoperative pancreatic protocol CT using dedicated software. The phenotype of pancreas on CT images was expressed with 478 radiomics features, which include the first order statistics, shape, texture, and texture features from wavelet and Laplacian of Gaussian filtering. The studies were randomly split into a training set (319 cases) and a testing set (164 cases). Feature reduction was performed by the minimum-redundancy maximum-relevance selection approach and random forest was applied for the 3-class classification. The overall classification accuracy of the testing set was 0.988 (162 among 164 cases were correctly classified). The sensitivity of PDAC and cyst was 0.968, 1.00, respectively. The specificity and PPV showed all 1.00. Most relevant features to differentiate 3 classes include intensity uniformity, shape compactness, and texture features of gray level non-uniformity, skewness, fractal dimension from the original images and filtered images. Radiomics features showed strong capability to differentiate pancreatic adenocarcinoma and cysts from normal pancreas with 3D segmented pancreas.

## New Imaging Techniques for the Male Urethra

Juan de Dios Berná-Mestre<sup>\*</sup>, Guillermo Carbonell, Thierry Balmaceda and Antonio Navarro

*Virgen de la Arrixaca University Hospital, Spain*

### Abstract

Introduction of contrast in urethrography was first done using clamp devices coupled to a syringe. These were replaced by the conventional technique using a Foley catheter. The drawbacks of this method are that it can cause pain on inflation of the balloon and it is not useful in cases with urethromeat alterations. Sonourethrography has been reported as being more accurate than urethrography for measuring urethral strictures and also for assessing the degree of spongiofibrosis. The purpose of this study is to describe "The Clamp Method" for performing urethrography, sonourethrography, MR and CT-urethrography.

**Material and Methods:** The present study describes a technique to optimize the imaging diagnosis of the male urethra, using a clamp device and a fine pre-lubricated catheter connected to a drip infusion system. A comparative study with the conventional technique of urethrography was performed. Another study was conducted to evaluate the clamp method for sonourethrography.

**Results:** Urethrography could not be performed with conventional technique in the 30 percent of the cases, while all the cases were performed by clamp method. Distressing pain was reported in most cases respect inflation of the balloon while no pain was reported in most cases respect external compression. Sonourethrography showed greater capacity for detecting strictures than urethrography.

**Conclusion:** The clamp method is simple and well tolerated by patients. It enables just one manipulator to perform sonourethrography. Sonographic contrast is necessary for voiding sonourethrography via the transperineal approach. The clamp method can also be used for CT-urethrography and MR- urethrography.

## **MRI-Guided Focused Ultrasound: A Transformative, State-of-the-Art Technology for 21<sup>st</sup> Century Medicine**

**Victor Frenkel**

*Department of Diagnostic Radiology and Nuclear Medicine, University of Maryland School of Medicine, Baltimore, MD, USA*

### **Abstract**

MRI-guided FUS (MRgFUS) is a new, disruptive technology allowing for controlled, targeted application of ultrasound energy deep within the body. Ultrasound energy can be tuned to create mechanical and/or thermal effects in tissues leading to a multitude of potential therapeutic benefits. These include thermal ablation, immune activation, and a host of transient structural effects that alter tissue permeability for improved delivery of therapeutics: small molecules, monoclonal antibodies, viral and non-viral gene vectors, nanoparticle drug carriers and even cells. MRgFUS is currently FDA-approved for thermal ablation of uterine fibroids, prostate and breast cancer, as well as palliative treatment of bone metastases. Most recently, it was approved for the treatment of Essential Tremor (ET). The noninvasive MRgFUS procedure for ET involves transcranial exposures for the ablation of the ventricular intermediate nucleus (VIM), located within the thalamus. The ability to safely treat the VIM for ET has created the opportunity to apply ultrasound for other brain-related applications, including enhanced therapeutic delivery. One of these is using MRgFUS to enhance delivery to invasive brain tumors (glioblastoma, GBM) by safely and reversibly opening the blood-brain barrier (BBB) in a selective spatial/temporal manner. This presentation will review the state-of-the-art MRgFUS technology in its current clinical use, followed by a review of our preclinical MRgFUS program and a discussion on how these treatments can enhance the delivery of both systemically and locally administered agents in the brain. Discussion will also include the underlying biophysical, ultrasound-tissue interactions involved for producing these effects.

## **PET Probes in Atheroma**

**John Buscombe**

*Cambridge University Hospitals, Cambridge, UK*

### **Abstract**

Our understanding of the pathophysiology of atheroma has widened the scope of imaging probes which can be used with positron emission tomography. The essential components of the vulnerable atheromatous plaque include inflammation, hypoxia and microcalcification.

Over the past 10 years the team at the Cambridge PET Center have utilized a number of probes to identify different aspects of the vulnerable plaque. The simplest of these probes is F-18 Fluorodeoxyglucose (FDG) which produces a strong signal in sites of inflammation. It has been shown to accumulate in sites of focal inflammation including major blood vessels such as the aorta where there is a strong correlation with sites of mechanical strain. Its use in coronary arteries has been limited by the adjacent activity within the normal myocardium. To overcome this, we have used gallium-68 (Ga-68) DOTATATE which attaches to the somatostatin receptors present on activated macrophages which allowed imaging of inflammatory plaques in coronary as well as peripheral arteries.

Calcification is often seen in atheroma it appears to represent a quiescent process but by using sodium fluoride (F-18 NaF) PET we can find areas of active calcification which correlates with new vulnerable atheroma. A further tool in our imaging toolbox has been F-18 fluoromisonidazole (FMISO) which we have shown to accumulate in the hypoxic heart of atheroma in the vulnerable plaque within the carotid arteries. Overall there is a new range of PET probes which are enabling us to explore the pathophysiology of atheroma in vivo.

## **Toward Patient-Specific Optimization of Post-Reconstruction Filtered OS-EM for Simultaneous-Acquisition Dual-Radionuclide Myocardial Perfusion SPECT**

**Xin Li\*, Abhinav K. Jha, Michael Ghaly, Fatma E. A. Elshahaby, Jonathan M. Links and Eric C. Frey**

*X-ray Inspection Lead Engineer, GE Global Research, Niskayuna, NY, USA*

### **Abstract**

Post-reconstruction filtered ordered subsets-expectation maximization (OS-EM) is widely used in myocardial perfusion

SPECT to allow for compensation for physical image degrading effects. It provides images with good quality if the reconstruction parameters are chosen appropriately. There have been a number of previous studies optimizing the reconstruction and filter in terms of performance of an anthropomorphic channelized hotelling observer (CHO). However, those efforts involved determining a single set of optimal parameters for an entire population. There is evidence that the optimal reconstruction parameters depend on characteristics of the imaging system and object imaged. We hypothesized that more patient-specific parameters could produce better task performance. In the study, we propose and evaluate a method for selecting patient-specific reconstruction parameters in the context of simultaneous dual-radionuclide myocardial perfusion SPECT. In this method, phantoms in a clinically representative XCAT phantom population were separated into three groups based on factors that can be easily estimated from the image data and were hypothesized to affect the optimal parameters. The factors used are parameters that were surrogates image resolution, image noise, and heart size. Using these factors, we separated the objects into three groups and found optimal parameters for each group. We also showed that the conventional CHO is not optimal for clinically realistic tasks where there is variation in signal and background. As a result, we developed a more optimal model observer strategy to evaluate image quality for such tasks. The results showed that the more patient-specific parameters did offer better task performance: using parameters optimized for the three groups resulted in overall better task performance than parameters optimized for the phantom population as a whole. The proposed model observer strategy and patient specific optimization idea can also be applied to other fields in medical imaging.

## Non-contrast T1 $\rho$ and Extracellular Volume Mapping for Characterizing Diffuse Myocardial Fibrosis in Spontaneous Type II Diabetes Rhesus Monkeys

Fabao Gao<sup>1,2\*</sup>, Wen Zeng<sup>2</sup>, Yu Zhang<sup>1</sup>, Li Gong<sup>2</sup> and Jie Zheng<sup>3</sup>

<sup>1</sup>Department of Radiology, West China Hospital of Sichuan University, China

<sup>2</sup>Sichuan Primed Shines Bio-tech Co., Ltd., China

<sup>3</sup>Mallinckrodt Institute of Radiology, Washington University School of Medicine in St. Louis, MO, USA

### Abstract

**Objectives:** To characterize the role of diffuse myocardial fibrosis in different degrees of diastolic dysfunction in spontaneous type II diabetes mellitus (T2DM) with non-invasive imaging biomarkers.

**Background:** Diastolic dysfunction (DD) is a pathophysiological cornerstone of the heart failure with preserved ejection fraction (HFpEF) syndrome. Diffuse myocardial fibrosis is thought to be a major contributor to DD, particularly in T2DM. However, the role of progressive diffuse fibrosis in DD in T2DM with HFpEF has not been fully investigated.

**Methods:** Eighteen spontaneous T2DM and nine healthy monkeys were studied. Echocardiography was performed on all monkeys for diastolic function classification (normal, mild, and moderate DD). We obtained cardiac magnetic resonance (CMR) imaging whole-heart cine, precontrast T1 and T1 $\rho$  maps at two different spin-locking frequencies, postcontrast T1 maps, and late gadolinium enhancement (LGE) images. We calculated extracellular volume fraction (ECV), and the myocardial fibrosis index (mFI) based on the dispersion characteristics of T1 $\rho$ . One T2DM monkey heart with moderate DD on was harvested for histopathological analysis.

**Results:** Echocardiographic results showed mild DD in nine T2DM monkeys ( $E/A < 1$ ,  $E'/A' > 1$ ,  $E' > 7$ ,  $E/E' < 11$ ) and moderate DD in the other 9 T2DM monkeys ( $E/A > 1$ ,  $E'/A' < 1$ ,  $E' < 7$ ,  $E/E' > 11$ ).  $E'$  correlated with mFI and ECV, respectively ( $r = -0.465$ ,  $p = 0.014$ ;  $r = -0.715$ ,  $p = 0.0001$ ). The mFI increased progressively from healthy to mild DD, and then to moderate DD ( $2.90 \pm 1.41$  vs.  $4.91 \pm 2.09$  vs.  $7.74 \pm 2.48$ ,  $p < 0.0001$ ). The differences between healthy and mild DD monkeys ( $p = 0.049$ ) or between mild and moderate DD monkeys ( $p = 0.007$ ) were all significant. The corresponding global ECV was also significant different between three groups of monkeys, but there was no significant different in ECV between healthy and mild monkeys. Histopathologic analysis showed that the myocardial extracellular space was widened with diffuse fibrosis (ECV = 37.46% and mFI = 5.85) in the monkey with moderate DD.

**Conclusions:** At the early to moderate stages of DD, diffuse myocardial fibrosis plays an important pathogenic role. Compared to ECV, mFI is a more sensitive imaging marker for the diagnosis of T2DM with mild DD.

## Myocardial T1-Mapping in Daily Cardiac Magnetic Resonance Study in Hypertrophic Cardiomyopathy

O. Yu. Dariy\*, S. A. Aleksandrova, V. N. Makarenko and L. A. Bokeria

A.N. Bakulev Scientific Center for Cardiovascular Surgery, Russia

## Abstract

**Objectives:** To optimize diagnosis algorithm in hypertrophic cardiomyopathy (HCM) using T1 mapping of myocardium. To estimate native T1, ECV and late gadolinium enhancement (LGE) segmentally and quantify their association with contractile dysfunction in the same segment in patients with HCM.

**Methods:** We performed 40 cardiac magnetic resonance studies on AchievaTX 3T scanner of HCM patients (n = 30) and (n = 10) control group. Modified Look-Locker Inversion Recovery (MOLLI) T1maps and LGE images were obtained for three slices in ventricular short axis plane before after the contrast agent injection. Assessment of T1 values and ECV values were based on 3 short axis slices, in areas where focal fibrosis was excluded. Analysis was carried out using CVI42 (Circle Cardiovascular Imaging Inc. Calgary, Canada). Statistical analysis was performed using Rang Correlation of Spearman.

**Results:** There were the maximum hypertrophy at the anterior- and posterior-septal segments of the basal myocardium, the minimum one at the apical segments. The native T1 value mean was around  $1317 \pm 94$ ms, significantly higher than the control group (native T1  $1093 \pm 23,7$ ms.). Mean ECV was  $29,8 \pm 4,5\%$ , higher than the control group also (ECV  $24,8 \pm 1,9\%$ ). We obtained individually association of every value (EDWT, native T1, LGE) with the strain values. The EDWT and native T1 had statistically significant association with circumferential (Ecc-FT) and radial (Err-FT) strain values ( $r = 0,5, < 0,0001$ ). Weak correlation of ECC-FT, Err-FT and ECV ( $r = 0,2, p > 0,05$ ). The LGE didn't have any statistically significant association with the strain values. The midwall fractional shortening and native T1 had weak correlation ( $r = 0,5 p > 0,05$ ).

**Conclusion:** The advent of absolute T1 measurement techniques allowed by definition of the ECV to quantify the entire range of fibrosis either diffuse or focal. We have found influence of contractile dysfunction of LV myocardium as with the degree of myocardial hypertrophy as with the native T1.

## Cerebral Mycotic Aneurysm and Infective Endocarditis: A Case Study

Leslie Wormely<sup>1\*</sup>, Arrin Williams<sup>1,2</sup> and Sashi Kilaru<sup>1</sup>

<sup>1</sup>The Christ Hospital Health Network, Cincinnati, OH, USA

<sup>2</sup>Mercy Hospital, Cincinnati, OH, USA

## Abstract

Mycotic aneurysms resulting from endocarditis are uncommon, and patients having aneurysms in multiple locations are rare. We report on a case of a patient having both infrapopliteal and cerebral mycotic aneurysms as a result of endocarditis. A patient was referred to the vascular lab for a lower extremity venous duplex, which incidentally demonstrated an infrapopliteal aneurysm of the right tibio-peroneal trunk. Computed tomography (CT) demonstrated two separate aneurysms: one at the origin of the anterior tibial artery and another involving the peroneal artery. The anterior tibial artery aneurysm was treated surgically. A transesophageal echocardiogram was performed on the patient and identified vegetation on the prosthetic aortic valve. The patient was then transferred to another facility for replacement of the prosthetic aortic valve. The patient suffered a cerebrovascular accident (CVA) postoperatively and subsequently had two cerebral mycotic aneurysms identified and treated.

## Intracranial Stents, Past Present and Future (Intracranial Angioplasty and Stenting for Cerebral Atherosclerosis; Result 106 Cases)

Daehyun Hwang

Department of Radiology, Seoul Paik Hospital, Inje University, Seoul, South Korea

## Abstract

**Background:** Stroke is most common cause of life threatening neurological disease and also it is leading cause of adult disability and third leading cause of death. Intracranial atherosclerosis is 8 to 10% of all ischemic strokes and reported poor outcome and high rate of morbidity and mortality.

**Materials and Methods:** We evaluated 108 consecutive patients (age mean 60.48, range 23-77 years, M : F = 59:49) who underwent intracranial stenting between March 2004 and December 2009. The location of lesion was anterior circulation (n = 70), MCA (n = 33), ICA (n = 37), posterior circulation (n = 38) and mean stenosis was 72.8%.

**Results:** The procedural success rate was 95.37%. 5 cases are unable to reach the target and performed Balloon angioplasty. There were overall three complications (2.77%) within period of follow up (six months); these included one minor strokes

(0.92%), and one deaths (0.92%), one restenosis (0.92%). The kind of stent was Endeavor (n = 45), Vision (n = 13), Cypher (n = 14), Neuroform (n = 5), Flexmaster (n = 9), Arthos pico (n = 6), Tsunami (n = 4), Guidant (n = 5), Abbott (n = 1), Jomed (n = 1).

**Conclusions:** In selected patients, endovascular revascularization of intracranial arteries with stent assisted angioplasty is technically feasible, effective and safe. Randomized multicenter trial comparing angioplasty and stenting with medical management alone must be performed.

## Radiological Evaluation of Aortopulmonary Window (APW): A Case Report

Abhishek Mashirkar\*, Bhavana Sonawane, Narendra Tembhekar and Atul Meshram

Department of Radiodiagnosis, Super Specialty Hospital and Government Medical College, Nagpur, India

### Abstract

**Background:** Aortopulmonary septal defect (APSD), also known as Aortopulmonary window (APW) is a congenital anomaly where there is an abnormal communication between the proximal aorta and the pulmonary trunk in the presence of separate aortic and pulmonary valves. Developmentally the defect results from incomplete separation of the common tube of the truncus arteriosus and the aortopulmonary trunk. Aortopulmonary septal defects occur in < 1% of all cardiac malformations.

M : F Ratio 1.8 : 1.

**Classification:** This classification separates APSD into four types

Type I: proximal APSD located just above the sinus of Valsalva, a few millimeters above the semilunar valve

Type II: distal APSD located in the uppermost portion of the ascending aorta

Type III: total defect involving the entire Aortopulmonary septum or ascending aorta

Type IV: intermediate defect

**Associations:** 50-70% of all patients with APSD are associated with other cardiac malformations

- Arch anomalies
- VSD
- ASD
- Right ventricular outflow tract anomalies
- Left ventricular outflow tract obstruction
- Transposition of the great arteries
- Coronary anomalies

**Aim:** Cardiac CT was performed to confirm the suspected diagnosis of APSD on 2D-echo.

**Material & Methods:** Cardiac CT scan done on 128 slice Toshiba Aquilion after IV contrast in a suspected case of APSD.

**Results and Conclusions:** A large communication filled with contrast is seen between ascending aorta and pulmonary artery s/o APSD (aorto pulmonary septal defect). Associated coronary anomaly is seen in the form of anomalous origin of RCA from MPA (ARCAPA). Right ventricular hypertrophy.

## Arterial Spin Labelling: Basics and Current Emerging Clinical Applications What Every Resident Must Know

Ram Mohan Vadapalli<sup>1\*</sup>, Abhinav Sriram Vadapalli<sup>2</sup>, Sita Jayalakshmi<sup>3</sup> and Manas Panigrahi<sup>3</sup>

<sup>1</sup>Consultant Radiologist, Vijaya Diagnostics, Hyderabad, India

<sup>2</sup>Armed Forces Medical College, Pune, India

<sup>3</sup>Krishna Institute of Medical Sciences, Hyderabad, India

### Abstract

**Introduction:** Arterial spin labelling (ASL) is a non-invasive, quantitative, repeatable MRI technique, which allows

measuring the brain perfusion without contrast agent using arterial blood water as an endogenous tracer and eliminating the risk of nephrogenic systemic fibrosis in patients with renal dysfunction. A radio frequency pulse (RF) using to invert the water molecules- this is the labelling part of the ASL.

After a delay (so-called post-labelling delay (PLD) or inversion times (TI)) the labelled blood flows into the brain tissue and a labelled image is acquired which contain signal from the inverted static tissue protons. A control image is also necessary without labelling. The difference between the control and labelled images provide a measure of labelled blood from arteries delivered to the tissue by perfusion.

**Content Organization:** Various techniques of arterial spin labelling (ASL) are discussed with their pearls and pitfalls. Role of ASL on following clinical applications are discussed, Acute and Chronic cerebrovascular disease, AV malformations, Neoplasms, Epilepsy, Neurodevelopmental disorders, Aging and Neurodegenerative disorders. Pediatric cerebral blood flow studies with perfusion based fMRI. Illustrative case examples are highlighted.

**Conclusion:** This educational review elucidates the emerging clinical application of ASL with illustrative examples.

## Granulomatous Mastitis a Mimicker on Elastography

Sandhya Dhankhar

Director & Consultant Radiologist, Faith Diagnostic Centre, Chandigarh, India

### Abstract

**Purpose:** To identify the characteristic features of granulomatous mastitis on ultrasound and how it mimics carcinoma breast. Elastography findings are exactly similar to a malignant lesion in breast and it is difficult to differentiate granulomatous mastitis from carcinoma breast on the basis of elastographic features. Hence, it is important to perform biopsy in lesions where there is strong clinical suspicion of granulomatous mastitis to confirm the diagnosis.

**Method and Materials:** 5 female patients were examined with history of lump in breast of 25-45 age groups and were subjected to sonography of breast or mammography of breast and then elastography was done in all patients to differentiate benign from malignant lesion. Strain elastography was performed on Epiq 7G Philips Ultrasound Machine and Strain ratio were obtained in all cases. Then these patients were subjected to either FNAC or Biopsy of the breast lesions.

**Results:** All the five patients had breast lump. Two patients had tenderness and three had just discomfort and no pain. The ultrasound and mammography features were mimicking the features of malignant lesion of breast, hence Strain Elastography was performed to differentiate these lesions. But on elastography all these lesions showed characteristic features of malignant mass lesion with Strain ratio as high as 8-9 which is seen in malignant lesions. Hence, it was difficult to differentiate Granulomatous mastitis from malignant breast lesion on the basis of ultrasound of breast and elastography of breast.

**Conclusion:** Elastography of breast does not help in patients of Granulomatous mastitis as findings mimic the features of malignant breast mass. FNAC or Biopsy is must in young patients with vague masses and where clinical suspicion of mastitis is there.

## Model-based Registration Approach for Image-Guided Surgery

Sungmin Kim<sup>1\*</sup> and Peter Kazanzides<sup>2</sup>

<sup>1</sup>Korea Institute of Machinery and Materials, Republic of Korea

<sup>2</sup>Johns Hopkins University, Baltimore, MD, USA

### Abstract

Image-guided surgery requires registration between an image coordinate system and patient coordinate system that is typically referenced to a tracking device. To do the registration, paired-point registration method is widely used, and this is achieved by localizing points (fiducials) in each coordinate system. Mostly, both localizations are performed manually on the screen (image coordinate) and the patient. These manual procedures introduce localization error that is user-dependent and can significantly decrease registration accuracy.

We propose the iterative closest touchable point (ICTP) registration framework, which uses model-based localization and a touchable region model. This method consists of three steps, fiducial marker localization, initial registration with paired-point registration, and fine registration based on the iterative closest point method.

The phantom experiments using a multi-modal fiducial marker that is commonly used in neurosurgery are conducted to evaluate the proposed ICTP registration framework. The results demonstrate that proposed method can provide accuracy improvements compared to the standard paired-point registration method, it's because the proposed method can reduce the effect of the surgeon's localization performance.

## MR-Venography in the Diagnosis of Post-Thrombotic Iliac Vein Obstruction and Extravascular Compression

V. Shebryakov<sup>1,2\*</sup>, Yu. Stoyko<sup>1</sup>, O. Bronov, M. Yashkin<sup>1</sup> and D. Lutarevich<sup>2</sup>

<sup>1</sup>K Pirogov National Medical & Surgical Center, Moscow, Russia

<sup>2</sup>Ramsay Diagnostics, Moscow, Russia

### Abstract

**Purpose:** Evaluate the information value of MRI in the diagnosis of post-thrombotic iliac vein obstruction and extravascular compression.

**Methods and Materials:** The study included 118 patients with CVD (clinical class C3-C6 according to the CEAP classification), including 47 men and 71 women. The average age of the patients was  $43.6 \pm 11.6$  years. Clinical classes of patients are as follows: C3 - 17, C4a - 8, C5 - 2, C6 - 1. All patients underwent ultrasound angio-scanning veins of the lower extremities and MRI of the iliac veins and inferior vena cava. Studies were performed on MRI using a special protocol contrast free sequences: 1. BH TROOFI/FIESTA ISO using Valsalva maneuver; 2. INHANCE 3D using free breathing technique, with subsequent 3D reconstruction.

**Results:** Eighty-seven patients have been diagnosed with stenosis of the left common iliac vein due to compression of the right common iliac artery (May-Turner syndrome). 21 patients underwent stenting of left common iliac vein with the May-Turner syndrome. Two patients underwent stenting of the left external and common iliac veins with post-thrombotic obstruction. 10 post-thrombotic deep vein changes have been revealed: post-thrombotic obliteration of the left common iliac vein (CIV) in 4 cases, right CIV, IVC in 3 cases, right external iliac vein (EIV) - 1, left EIV - 1, 1 with stenosis of both EIV, 2 stenosis of the left CFV and 1 has demonstrated complete recanalization of the left EIV after thrombosis of a previously deferred.

**Conclusion:** MR-venography is the most optimal method in the diagnosis of the causes of extra and intravenous pathology of the IVC and its basin. There is no radiation exposure, non-contrast agent and short time relation. 3D-reconstruction of the IVC and iliac veins can be used for planning corrective and reconstructive operations.

## Generalized Giant Cell Arteritis Discovered on Positron Emission Tomography

Amit Habbu<sup>1\*</sup>, Kalpita Hatti<sup>1</sup>, Luke Lancaster<sup>2</sup>, Nicholar Hendricks<sup>2</sup>, William Grosh<sup>3</sup> and Janet Lewis<sup>4</sup>

<sup>1</sup>Department of Radiology, Kadlec Regional Medical Center, Richland, WA, USA

<sup>2</sup>Department of Radiology, University of Virginia, Charlottesville, VA, USA

<sup>3</sup>Division of Hematology and Oncology, University of Virginia, Charlottesville, VA, USA

<sup>4</sup>Division of Rheumatology, University of Virginia, Charlottesville, VA, USA

### Abstract

An 82-year-old man with a remote history of metastatic melanoma status post chemotherapy presented with fatigue, generalized weakness, low grade fevers, abdominal pain and weight loss. Positron emission tomography (PET) scan was obtained, which revealed diffuse and symmetric increased F-18 Fluorodeoxyglucose (FDG) uptake throughout the large arterial vasculature in the neck, chest, abdomen, pelvis and lower extremities. CT angiogram showed subtle wall thickening involving the bilateral vertebral, bilateral axillary, left subclavian, abdominal aorta, bilateral common iliac, internal iliac, common femoral, superficial femoral, popliteal and anterior tibial arteries, consistent with large vessel vasculitis. Subsequent left temporal artery biopsy revealed multiple giant cells with associated lymphoid cells infiltrating all levels of the artery, but most focused in the media and adventitia, consistent with giant cell arteritis (GCA). The patient was started on prednisone, resulting in prompt improvement in his constitutional symptoms and normalization of his sedimentation rate. PET scan appears to be an emerging and promising imaging technique for early detection and subsequent monitoring of treatment success of large-vessel inflammation in giant cell arteritis. PET-CT has been demonstrated to have 85% sensitivity and 83% specificity for active large vessel vasculitis. The current literature supports increasing utility of this modality as an adjunct in diagnosing and monitoring

this disease.

## Sonourethrograph: Role in the Evaluation of Anterior Urethral Strictures

Abhishek Mashirkar\*, Bhavana Sonawane, Narendra Tembhekar, Atul Meshram

Department of Radiodiagnosis, Super Specialty Hospital and Government Medical College, Nagpur, India

### Abstract

**Aim:** To assess the role of sonourethrography in evaluation of anterior urethral abnormalities (specially strictures). Staging & grading of anterior urethral strictures. To assess the extent of spongiosal and periurethral involvement in cases of urethral strictures. To compare the efficacy of sonourethrography as compared to conventional retrograde urography. Role of sonourethrography in management & follow-up of anterior urethral disorders (specially strictures).

**Methods:** A study of 70 patients were carried in the Department of Radio-diagnosis, SSH and GMC Nagpur, India. Patients from all the age groups referred at our institute/department.

**Results:** Of the 70 patients who underwent sonourethrograph 33 patients were diagnosed to have 39 strictures out of these 39 strictures, 2 strictures are mild (5.12%), 16 as moderate (41.02%) & 21 as severe (53.84%). 20 strictures were short (focal) while 13 were long (diffuse).

**Conclusions:** Sonourethrography is useful for diagnosis of anterior urethral pathologies. Compared with conventional retrograde urethrography (RGU), sonourethrography is equally necessary in detecting anterior urethral pathologies. Useful in stricture classification, calculus & other soft tissue lesion detection. Color doppler evaluation of periurethral vessels for guidance of surgeons can avoid damage to the periurethral vessels.

**Discussion:** Some findings are better visualized on SUG than RGU such as, periurethral fibrosis, urethral calculi, mucosal thickening, mucosal flap also more sensitive in detecting mild and moderate variety of urethritis than retrograde urethrograph. Most patient (85%) said they preferred SUG over RUG.

## Ultrasound for Diaphragmatic Dysfunction in Post-Operative Cardiac Children

Hussam K. Hamadah<sup>1</sup>\*, Mohamed S. Kabbani<sup>1,2</sup>, Mahmoud Elbarbary<sup>1,2</sup> and Omar Hijazi<sup>1,2</sup>

<sup>1</sup>Section of Pediatric Cardiac ICU, King Abdulaziz Cardiac Center, King Abdulaziz Medical City, Ministry of National Guard-Health Affairs, Riyadh, Kingdom of Saudi Arabia

<sup>2</sup>King Saud bin Abdulaziz University for Health Sciences, Riyadh, Kingdom of Saudi Arabia

### Abstract

The use of ultrasound for assessment of diaphragmatic dysfunction after pediatric cardiac surgery may be underutilized. This study aims to evaluate the role of bedside ultrasound performed by an intensivist to diagnose diaphragmatic dysfunction and the need for plication after pediatric cardiac surgery.

**Methods:** Retrospective cohort study on prospectively collected data for postoperative children admitted to pediatric cardiac ICU (PCICU) during 2013. Diaphragmatic dysfunction was suspected based on difficulties in weaning from positive pressure ventilation or chest X-ray findings. Ultrasound studies were performed by PCICU intensivist and confirmed by qualified radiologist.

**Results:** Out of 344 post-operative patients, 32 needed diaphragm ultrasounds for suspected dysfunction. Ultrasound confirmed diaphragmatic dysfunction in 17/32 (53%) patients with an average age and weight of  $10.8 \pm 3.8$  months and  $6 \pm 1$  kg respectively. The incidence rate of diaphragmatic dysfunction was 4.9% in relation to the whole population. Diaphragmatic plication was needed in 9/17 cases (53%), with rate of 2.6% in post-operative cardiac children. Mean plication day was  $15.1 \pm 1.3$  days after surgery. All patients who underwent plication were under 4 months of age. Post plication, they were discharged with mean PCICU and hospital stay of  $19 \pm 3.5$  and  $42 \pm 8$  days respectively.

**Conclusions:** Critical care ultrasound assessment of diaphragmatic movement is a useful and practical bedside tool that can be performed by a trained PCICU intensivist. It may help in early detection and management of diaphragmatic dysfunction post pediatric cardiac surgery through a decision-making algorithm that may have potential positive effect on morbidity and outcome.

## Poster Presentations

### Septic Emboli in Lungs from Tricuspid Valve Endocarditis

Arnav Wadhawan<sup>1</sup> and Rajinder Bajwa<sup>2</sup>

<sup>1</sup>Ridley College, Ontario, Canada

<sup>2</sup>Niagara Falls Memorial Medical Center, Niagara Falls, NY, USA

#### Abstract

28-year-old female with history of intravenous drug use admitted to hospital with sudden onset chest pain and shortness of breath. Blood cultures grew Methicillin Resistant *Staphylococcus aureus*. Trans-thoracic echocardiogram showed 0.5 cm vegetation on tricuspid valve. CT scan of chest showed multiple pleural based opacities in the lungs. Some of this showed cavitation. In given scenario patient was diagnosed with right sided infective endocarditis along with septic emboli. She was treated with 6 weeks of IV vancomycin. Patient responded well to medical treatment.

### Acute Carotid Thrombosis and Ischemic Stroke Following Overdose of the Synthetic Cannabinoid K2 in a Previously Healthy Young Adult Male

Joseph Bibawy<sup>1</sup>, Raihan Faroqui, Peter Mena, Allen R. Wolfe, George A. Visvikis and Michael T. Mantello

*Richmond University Medical Center, Staten Island, NY, USA*

#### Abstract

With the popularity of synthetic cannabinoid street drugs such as “K2 and Spice,” a number of serious neurologic adverse events are coming to light. This case is of a 36-year-old African American male, with no significant medical history, who presented with extensive left cervical and intracranial internal carotid artery occlusion and subsequent ischemic stroke. The patient endorsed smoking K2-a synthetic cannabinoid (SC) with structural similarity to cannabis. The mechanism by which SC abuse induces a prothrombotic state leading to ischemic neurovascular sequelae is currently unclear, although a temporal association in the absence of other stroke risk factors suggests a causal relationship. Our case highlights the need for emergent neuroimaging upon suspected SC overdose. Practitioners should be vigilant in recognizing that ischemic stroke and unexplained neurologic deficit can arise after SC abuse, especially in younger populations with few stroke risk factors and who are prone to chronic cannabis use.

### Deep-Learned Generation of Synthetic X-Rays from Segmentations

Nicholas Chedid<sup>1</sup>, Praneeth Satta<sup>1</sup> and Richard Andrew Taylor<sup>2</sup>

<sup>1</sup>Yale School of Medicine, New Haven, CT

<sup>2</sup>Department of Emergency Medicine, Yale School of Medicine, New Haven, CT, USA

#### Abstract

**Purpose:** Fractures are a very common reason for emergency department visits. Some fractures are easily discernable on x-ray, but others are subtle and require a radiologist’s inspection. Any technology that can automatically detect fractures has the potential to reduce emergency department waiting times. However, training image analysis algorithms often requires hundreds or thousands of manually annotated examples. Here, we describe a method of creating synthetic X-rays from procedurally-generated segmentations, thereby creating an annotated dataset with minimal human time expenditure.

**Methods:** 50 X-rays of femoral fractures were obtained from an internet search. 200 segmentations were generated programmatically by drawings arcs and lines to represent bone shapes (Figure 1B). A cyclic generative adversarial neural network (CycleGAN) is a form of neural network that can be trained to synthesize images of a certain appearance from arbitrary input data. A CycleGAN was trained to synthesize X-rays from the procedural segmentations. The training dataset was assembled by randomly pairing each of the 200 segmentations with one of the 50 true X-ray images. These pairings were redefined at each epoch. Training lasted 200 epochs.

**Results:** The trained network was able to synthesize realistic X-ray images that mirrored the structure of the input

segmentations (Figure 1C).

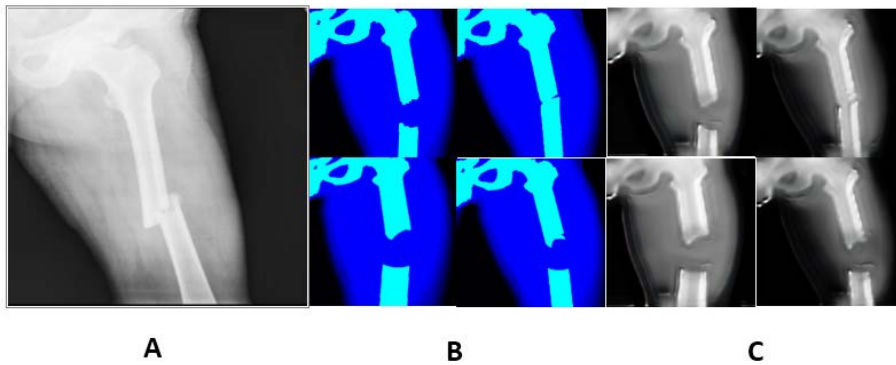


**Figure 1:** A. A true real x-ray image. B. Procedurally-generated segmentations. C. Synthetic X-rays generated from the procedural segmentations using a CycleGAN.

**Conclusion:** It is possible to synthesize realistic x-rays from procedurally generated segmentations. This could be a valuable method of generating training data for X-ray segmentation algorithms.

## Virtual Presentations

### Simple Diagrammatic Approach to Delineate Duodenum on a Radiotherapy Planning CT Scan

Trinanjana Basu

Consultant Radiation Oncologist, HCG Apex Cancer Centre, Mumbai, India

#### Abstract

**Background:** In recent years there has been increasing application of intensity modulated radiotherapy (IMRT) and stereotactic body radiotherapy (SBRT) for the treatment of abdominal malignancies (stomach, pancreas, liver, spinal metastases) which warrants accurate delineation of organs at risk (OAR) especially duodenum. This pictorial essay following the RTOG guideline elaborates the step by step identification of the different parts duodenum in relation to the adjoining important structures.

**Materials and Methods:** Using radiotherapy planning CT scan (RTP) with 1.25 mm slice thickness and IV contrast in axial CT sections different parts of duodenum are marked with help of adjoining structures like stomach, liver, lumbar vertebrae pancreas, spleen and both kidneys. The main aim was to delineate and reproduce in systematic manner.

**Results:** Different steps are drawn and demonstrated in pictorial presentation.

**Conclusion:** This was first of its kind easy and reproducible delineation of duodenum on a radiotherapy planning CT scan. Future studies aiming at differential motion and margin (Already published as abstract in ESTRO 2016) are underway.

### Virtual Bronchoscopy Multislice Tomography in Traumatic Injuries of the Main Bronchi

Petr Mikhailovich Kotlyarov and Natalia Vasilievna Chernichenko

Russian scientific center of X-ray radiology, Moscow, Russia

#### Abstract

The analysis of virtual bronchoscopy data was carried out in 7 patients with traumatic injuries of one of the main bronchi as a result of thoracic injuries. Patients underwent reconstructive surgery - isolated resection of the main bronchus with the imposition of tracheobronchial anastomosis. MSCT with bolus amplification was performed on 320-slice unit with data

processing on a workstation. The data of native MSCT, VB fly through were supplemented with 3D-volumetric, multiplanar reconstructions, MinIP mode. VB data were compared through the results of bronchoscopy. In the MSCT, on the side of the lesion, hemo and pneumothorax, fractures of the ribs, sternum, vertebral bodies, subcutaneous emphysema, and VB revealed various localization of the break in the main bronchus, through the lumen of which the chest cavity with the collapsed lung and liquid level was traced. The zone of rupture of the main bronchus was visualized below the trachea bifurcation for 4-36 mm, lumen of the main and other bronchi was not visualized. 3D-volumetric, multiplanar reconstructions, the tracheobronchial system MinIP mode supplemented the data of MSCT and VB fly through. The VB data coincided with the bronchoscopy results. Postoperative MSCT determined complete restoration of ventilation of the damaged lung, deformation of the lumen of bronchus in the area of reconstructive intervention. VB clearly revealed the place of bronchial reconstruction, cicatricial changes in the bronchus and coincided with the bronchoscopy. Thus, VB MSCT allows you to accurately determine the damage to the main bronchi, to monitor the effectiveness of reconstructive operations.

## **Possibilities of Multislice Computed Tomography for the Detection of Malignant Tumors of the Retroperitoneal Space and Control of Their Treatment in Children**

**Elena Lomova<sup>\*</sup> and S. A. Dudkin**

*Novokuznetsk City Children's Clinical Hospital No. 4, Novokuznetsk, Russia*

### **Abstract**

Among the many retroperitoneal tumors in children, the most common tumor is Wilms and neuroblastoma. The standard of treatment for these patients is surgery. Taking into account the development of chemotherapy in the approaches to the treatment of these diseases, the results of the latter have significantly improved. Survival of almost 100% determines the diagnosis in the first year of life, which corresponds to a small stage of the disease and the effectiveness of training, and in some cases in children up to a year with neuroblastoma without the N-myc gene, is possible only observation. Even from these shortened postulates of therapy of the above tumors, it is clear that the primary radiation diagnosis is the first and most important element, sometimes allowing, like a Wilms tumor, to begin pre-operative treatment even without biopsy.

## **Use of Radiopharmaceuticals Based on $^{99m}\text{Tc}$ in Estimation of the Bone Metastatic Damage by Results of Scintigraphy and SPECT/CT Bones of the Skeleton. Analysis of Practical Work of the Nuclear Medicine Department**

**Maira Kalabayeva, Yekaterina Lyugay<sup>\*</sup> and Aigul Saduakassova**

*Hospital of Medical Center Office of the Department of the Presidential Affairs of the Republic of Kazakhstan, Nazarbayev University, Kazakhstan*

### **Abstract**

One of the most common localizations of metastatic lesions is the skeletal system. The presence or absence of metastases in the bones of the skeleton is a key issue in making clinical decisions. Numerous methods are used to detect metastatic lesions, including studies of scintigraphy and SPECT/CT of the bones of the skeleton. An integral part of the work in radioisotope diagnostics is the analysis of studies with different radiopharmaceuticals for obtaining optimal results for the use of various radiopharmaceuticals.

The goal of the work is to evaluate the results of scintigraphy and SPECT/CT studies of skeletal bones performed using various radiopharmaceuticals with  $^{99m}\text{Tc}$  complexes, as well as analysis of the results of studies used in the clinical practice of the Hospital.

The number of patients during the study period is 169 people in 2015-2018 years. This group of patients is the main research group. Based on the analysis of the diagnostic cycle in this group, the diagnostic effectiveness of bone metastases will be determined in patients with different oncology diseases.

## Breast Tomosynthesis: A Comparison Study Between Commercial Imaging System and Phase Sensitive Imaging Using Synchrotron Radiation

Anastasia Daskalaki<sup>1</sup>, Gerasimos A.T. Messaris<sup>2</sup> and Nicolas Pallikarakis<sup>1</sup>

<sup>1</sup>Biomedical Technology Unit, School of Medicine, University of Patras, Patras, Greece

<sup>2</sup>Department of Medical Physics, University Hospital of Patras, Patras, Greece

### Abstract

The main goal of this study is to examine the potential advantages of phase sensitive imaging in breast tomosynthesis (BT) for accurate and early detection of breast cancer. An in-house phantom with 5 cm radius and 3 cm thickness of paraffin wax with embedded spheres, fibers and CaCO<sub>3</sub> powder simulating breast malignancies was used. BT images were acquired with an in-line phase contrast mode using synchrotron radiation at 20 keV. Fifteen projections were obtained with an object to detector distance 150 cm an acquisition arc of 15° and a mean glandular dose (MGD) of 2.4 mGy. Attenuation based BT images of the same phantom were acquired with the use of a commercial imaging system. In this case, 15 projections were obtained at 28 kVp, 35 mAs with MGD 2.45 mGy, within an acquisition arc of 15°. In both experiments a filtered back projection reconstruction algorithm was used, resulting in BT planes of 1 mm distance. The reconstructed planes of the two experiments were compared visually and quantitatively. The edges of the main mammographic structures appeared to be sharper in the case of phase contrast imaging, making their detectability easier. Line profiles and contrast to noise ratio values confirmed the improvement of phase contrast BT over conventional BT imaging.

### PRF in Dentistry

Mohammed Jasim Al-Juboori

Lecturer, Department of Periodontology, Al-Rafidain College, Baghdad, Iraq

### Abstract

Platelet-rich fibrin (PRF) belongs to a new generation of platelet concentrates geared to simplified preparation without biochemical blood additives. Concentrates is recent, and its efficiency remains controversial. During PRF processing by centrifugation, platelets are activated, and their massive degranulation implies a very significant cytokine release. Concentrated platelet-rich plasma platelet cytokines have already been quantified in many technologic configurations. This result would imply that PRF, unlike the other platelet concentrates, would be able to release cytokines during fibrin matrix remodeling; like mechanism might explain the clinically observed healing properties of PRF.

The event of wound healing that PRF might participate are: angiogenesis, immune control, circulating stem cells trapping, and wound-covering epithelialization. All of the known clinical applications of PRF highlight an accelerated tissue cicatrization due to the development of effective neovascularization, accelerated wound closing with rapid tissue remodelling, and nearly total absence of infectious events. In our presentation we are going to highlight the effect of PRF in oral tissue healing and its various usage in the oral surgical procedure with documented cases. These cases will show the usage of PRF in guided bone regeneration, sinus lifting, socket closure, gingival recession, oro-antral fistula closure and connective tissue donor site coverage.

**Citation:** Proceedings of the First International Conference on Medical Imaging and Case Reports (MICR-2018). *J Med Imaging Case Rep* 2(Suppl 1): S1-S27.

**Copyright:** This is an Open Access article distributed under the terms of the Creative Commons Attribution 4.0 International License (CC-BY) (<http://creativecommons.org/licenses/by/4.0/>) which permits commercial use, including reproduction, adaptation, and distribution of the article provided the original author and source are credited. Published by United Scientific Group.

**Received:** November 08, 2018 **Accepted:** November 18, 2018 **Published:** November 25, 2018